

CALIFORNIA PATH PROGRAM  
INSTITUTE OF TRANSPORTATION STUDIES  
UNIVERSITY OF CALIFORNIA, BERKELEY

# **Vehicle Modeling and Verification of CNG-Powered Transit Buses**

**J.K. Hedrick, A. Ni**

**California PATH Working Paper  
UCB-ITS-PWP-2004-3**

This work was performed as part of the California PATH Program of the University of California, in cooperation with the State of California Business, Transportation, and Housing Agency, Department of Transportation; and the United States Department Transportation, Federal Highway Administration.

The contents of this report reflect the views of the authors who are responsible for the facts and the accuracy of the data presented herein. The contents do not necessarily reflect the official views or policies of the State of California. This report does not constitute a standard, specification, or regulation.

Final Report for Task Order 4206

February 2004

ISSN 1055-1417

# **Vehicle Modeling and Verification of CNG-Powered Transit Buses**

Annual Report

PATH Task Order 4206

J.K. Hedrick  
A. Ni

Mechanical Engineering Department  
University of California at Berkeley  
Berkeley, CA 94720

# Contents

- 1 Introduction** **1**
  
- 2 Modeling** **3**
  - 2.1 Vehicle Dynamics ..... 3
    - 2.1.1 Torque Converter Modes ..... 3
    - 2.1.2 Model ..... 5
      - 2.1.2.1 Locked Vehicle Dynamics ..... 5
      - 2.1.2.2 Unlocked Vehicle Dynamics ..... 6
      - 2.1.2.3 Switching between the two ..... 8
    - 2.1.3 Tuning Methodology ..... 8
      - 2.1.3.1 Locked Dynamics ..... 8
      - 2.1.3.2 Unlocked Vehicle Dynamics ..... 10
  - 2.2 Gear Shift ..... 11
  - 2.3 Engine ..... 13
  
- 3 Simulation Analysis** **16**
  - 3.1 Vehicle Dynamics ..... 16
  - 3.2 Vehicle Dynamics and Gear Shifts ..... 17
  - 3.3 Complete Simulation (VD, Gear Shifts, Torque Mapping) ..... 19
  - 3.4 Future Work ..... 20
  
- 4 Summary and Conclusions** **22**

# List of Figures

1.1	PATH Transit Bus Powered by Compressed Natural Gas . . . . .	2
2.1	Internal Diagram of a Torque Converter . . . . .	4
2.2	Discrepancy between Crow's Landing Testing Directions . . . . .	9
2.3	Sample Fit of Calculated Pump Torque . . . . .	11
2.4	Gear Shifting Points . . . . .	12
2.5	Engine Speed and Torque at Constant 38.78% Throttle Input . . . . .	14
2.5	Engine Maps for (a) First Gear and (b) Higher Gears . . . . .	14
3.1	Step Response with Vehicle Dynamics Simulation . . . . .	17
3.2	Step Response with Vehicle Dynamics and Gear Shift Simulation . . . . .	18
3.3	Step Response with Full Simulation . . . . .	19
3.4	Torque Signals for the 98.4% Step Response . . . . .	20

# Chapter 1

## Introduction

Automated highway systems (AHS) research has mainly focused on passenger vehicle automation, but growing attention has been given to heavy duty vehicles for a number of reasons. Heavy duty vehicles spend a large amount of time in operation, so even small improvements in performance can have significant impact. Second, unlike passenger vehicles, the relative costs of installing on-vehicle technology for AHS operation in heavy duty vehicles are minimal. Finally, automation of the entire range of vehicle types and sizes need to be studied in order to understand the effects of mixed vehicle traffic on the safety and performance of the AHS [1].

In order to successfully automate the control of any vehicle, it is first imperative to have a mathematical model that accurately describes the behavior of the vehicle. With more accurate models, better control algorithms can be used. In the California Partners for Advanced Transit and Highways (PATH) program, models exist for some heavy duty vehicles like their diesel-powered trucks, but none have been developed for their transit buses powered by compressed natural gas (CNG) engines.

This report will present the results of the initial study to develop an accurate working model of the 40 foot New Flyer Bus powered by the Cummins C8.3+ 280G CNG engine (Figure 1.1). The main focus of the study is the modeling of the vehicle dynamics using step input acceleration data. Other parts of the research include gear shifting and torque production from the CNG engine, all of which are required to produce a completely simulation-capable bus model.



Figure 1.1: PATH Transit Bus Powered by Compressed Natural Gas

The remainder of the report will be organized as follows. First, the developed model will be presented along with the tuning methods use to obtain the parameters to fit the model. Then, resulting simulations will be analyzed, comparing the model to actual driving data. Finally, the results will be summarized in the conclusion.

# Chapter 2

## Modeling

The models presented in this section are developed primarily from step input driving data from the New Flyer Bus, commanded both manually and electronically. The bus was run both directions on the airstrip at PATH's testing facility at Crow's Landing, California. Data is collected through the onboard JBus instrumentation.

This section will present and discuss the models developed in the study. The model is organized into three sections: vehicle dynamics, gear shifting, and engine dynamics.

### 2.1 Vehicle Dynamics

The generalized vehicle dynamics are divided into two very different modes: one when the torque converter is locked and one when it is unlocked. Before the model is presented, it is necessary to understand the torque converter—why it has these different modes, and how it affects the dynamics of the vehicle. After the model is presented, a section is dedicated to the tuning methodology used to come about the model's parameters.

#### 2.1.1 Torque Converter Modes

The torque converter is a part of the automatic transmission, the Allison B400R, and acts as the automatic analog to a clutch in a manual transmission. The torque converter provides a fluidic coupling between the engine

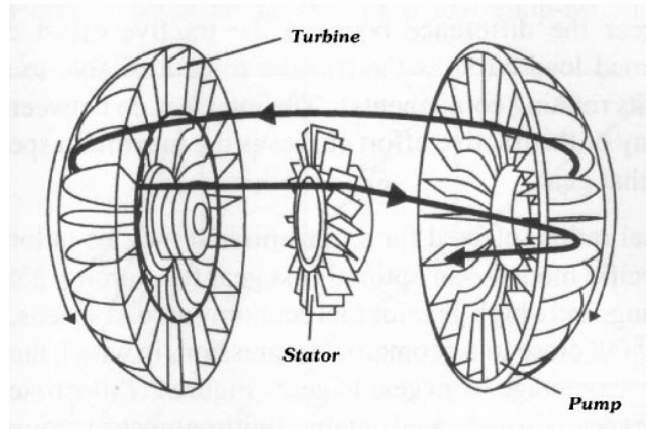


Figure 2.1: Internal Diagram of a Torque Converter [1]

shaft and gear set. Figure 2.1 shows the internals of a torque converter. The pump is rotated by the crankshaft in the engine, which generates a torque on the turbine by spinning the fluid onto the turbine blades. Any backflow is redirected by the stator to assist in driving the turbine [1]. By using a fluidic coupling such as this, the engine is able to idle when the bus is stopped without stalling, because the pump can rotate at idle speed while creating only a little torque on the turbine, at which time the vehicle can be held stationary by the bus's brakes. It is this 'slipping' of the torque converter that allows for differences in motor and wheel speeds, but this same ability can also lead to power loss, i.e. if the torque converter slips during normal higher speed driving. For this reason, the torque converter is given the ability to enter a 'locked mode,' where a hard connection ensures that the pump and turbine rotate at the same speed. This occurs after the vehicle reaches a certain speed. In the Allison B400R the torque converter locks during acceleration at 18.5 miles per hour and unlocks during deceleration at 16.0 miles per hour [2]. It is because of this locking that there arises two significantly differently sets of vehicle dynamics that need to be examined independently.

Parameter	Description	value (if constant)
$R_g$	overall gear ratio	
$\tau_{eng}$	engine torque	
$\theta$	road grade	
$\tau_{brake}$	brake torque	
$v$	vehicle velocity	
$v_{hw}$	headwind velocity	
$g$	gravitational acceleration	9.81 $m/s^2$
$m$	vehicle mass	13541 $kg$
$h$	wheel radius	0.4775 $m$
$F_{roll}$	rolling resistance	1930 $N$
$C_{aero}$	aerodynamic drag	3.21 $kg/m$
$I_{wheel}$	wheel inertia	38.3 $kg-m^2$
$I_{eng}$	engine inertia	1.88 $kg-m^2$

Table 2.1: Vehicle Dynamics Model Parameters, Descriptions, and Values

## 2.1.2 Model

The description of the vehicle dynamics model will be split up into the locked mode and then the unlocked mode. Then, a section will be dedicated to describing considerations necessary for switching between the modes during simulation. For convenience and clarity, Table 2.1 lists the symbols of model parameters (and value, if applicable) used in equations in this report.

### 2.1.2.1 Locked Vehicle Dynamics

At high speeds, the vehicle dynamics are simpler than at lower speeds because there is no slipping in the torque converter. The motion of the bus is governed by Equation 2.1, modified from Song et al. [3]

$$\dot{v} = R_g h \left[ \frac{\tau_{eng} - R_g (mgh \sin \theta + \tau_{brake} + F_{roll} h + (v + v_{hw})^2 C_{aero} h)}{R_g^2 (6I_{wheel} + mh^2) + I_{eng}} \right] \quad (2.1)$$

This is fundamentally Newton's second law, deriving acceleration from the sum of the torques on the bus (due to engine, road grade, brakes, rolling resistance, drag) and the effective inertia (from mass of vehicle, inertia of the wheels and engine). The engine speed is then calculated from the vehicle velocity.

$$\omega_e = \frac{v}{R_g h} \quad (2.2)$$

Of special note is the part of Equation 2.1 relating to aerodynamics, modified from [3] to incorporate the presence of wind disturbance. The force on the bus resulting from wind resistance is

$$F_{wind} = (v + v_{hw})^2 C_{aero} \quad (2.3)$$

where  $C_{aero}$  is derived from

$$C_{aero} = \frac{\rho C_d A_f}{2} \quad (2.4)$$

$\rho$  is the density of air,  $C_d$  the drag coefficient (0.6), and  $A_f$  is the frontal area of the bus (2.44 meters by 3.35 meters). Equation 2.3 adds the  $v_{hw}$  term, so that the wind plays a factor in the drag. A tailwind is expressed as a negative  $v_{hw}$  value.

### 2.1.2.2 Unlocked Vehicle Dynamics

When the torque converter is unlocked during low-speed driving, the dynamics become more complicated. The empirical model used for modeling the torque converter is modified from Kotwicki's input-output mapping between the speeds and torques of the pump and torque [4].

$$\tau_{pump}(\omega_p, \omega_t) = p_1 \omega_p^2 + p_2 \omega_p \omega_t + p_3 \omega_t^2 + p_4 \quad (2.5)$$

$$\tau_{turb}(\omega_p, \omega_t) = t_1 \omega_p^2 + t_2 \omega_p \omega_t + t_3 \omega_t^2 + t_4 \quad (2.6)$$

Pump			Turbine		
	uncoupled	coupled		uncoupled	coupled
$p_1$	3.09e-2	-1.26e-1	$t_1$	9.24e-2	5.69e-1
$p_2$	-1.74e-2	4.07e-1	$t_2$	-1.71e-1	-1.05
$p_3$	-4.41e-3	-2.83e-1	$t_3$	9.63e-2	4.86e1
$p_4$	1.91	10.5	$t_4$	12.9	0.00

Table 2.2: Torque Converter Fit Parameters

Equations 2.5 and 2.6 describe the torques on both sides of the torque converter when the torque converter is unlocked. Like the torque converter of PATH's diesel trucks, two different sets of fits are required: one for when the speed ratio,  $\omega_t/\omega_p$ , is below 0.9, and one for when it is equal to or above 0.9. These are called the uncoupled and coupled modes of the torque converter, respectively. The values of the fits are listed in Table 2.2. The pump is the side of the torque converter connected to the engine's crankshaft, and  $\tau_{pump}$  is the torque that the pump in the torque converter applies to the fluid. The derivative of the engine speed, engine acceleration is given by the equation

$$\dot{\omega}_e = \frac{\tau_{eng} - \tau_{pump}}{I_e} \quad (2.7)$$

On the other side of the torque converter,  $\tau_{turb}$  is the torque associated with the fluid impacting onto the turbine. This relates to the overall acceleration of the vehicle by the following:

$$\dot{v} = R_g h \left[ \frac{\tau_{turb} - R_g (mgh \sin \theta + \tau_{brake} + F_{roll} h + (v + v_{hw})^2 C_{aero} h)}{R_g^2 (6I_{wheel} + mh^2) + I_{eng}} \right] \quad (2.8)$$

Note that Equation 2.8 is simply Equation 2.1 with  $\tau_{turb}$  substituted in place of  $\tau_{eng}$ . In the locked version of the vehicle dynamics, the torque from the engine travels straight through the torque converter to the vehicle (minus driveline inefficiencies and geared appropriately). In the unlocked version, the engine

torque drives the pump of the torque converter, which uses the fluid to transmit the torque to the turbine and the rest of the vehicle.

### *2.1.2.3 Switching Between the Modes*

In the locked torque converter mode, vehicle acceleration is integrated to obtain vehicle speed. Engine speed is then calculated from vehicle speed. In the unlocked mode, engine acceleration is integrated to obtain engine speed. When switching from one mode to the other in simulation, it is important to transfer the initial conditions so that the integrations can be done correctly. When switching from unlocked to locked mode, the initial condition of vehicle speed is needed. When switching from locked to unlocked, the initial condition of both vehicle speed and engine speed is required. In this case, the engine speed can be calculated from the vehicle speed, as they are directly correlated in the locked mode, which is where they came from.

## **2.1.3 Tuning Methodology**

This section describes the steps taken and methods used in developing the bus model from the data taken from Crow's Landing. These steps can be retraced if it is found that retuning of model parameters is necessary.

### *2.1.3.1 Locked Dynamics*

Before any work can be done to find the characteristics of the torque converter, it is necessary to identify the parameters of the simpler vehicle dynamics in the locked torque converter mode. This means loading as much external JBus data as possible – engine torque, gear shifts, as well as the data of the unlocked mode dynamics.

Step responses start the vehicle off at zero speed, so the data begins in the unlocked torque converter mode; it necessary to load unlocked vehicle data. This allows for the correct initial conditions to be available for integration once the vehicle reaches locking speed. From [2], all constant parameters in Table 2.2 are known, except for  $F_{roll}$  and  $I_{wheel}$ .  $C_{aero}$  is tunable also, because it is a sensitive parameter consisting of many variables and is

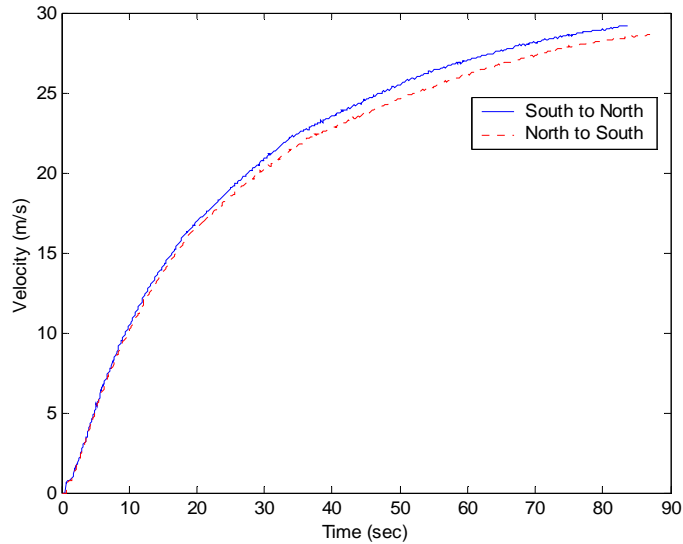


Figure 2.2: Discrepancy between Crow’s Landing Testing Directions

hard to measure accurately. Information for  $I_{wheel}$  is not available, so the value listed is taken from PATH’s diesel truck wheels. In Equation 2.1, the value of  $I_{wheel}$  is insignificant in comparison to the mass of the whole vehicle. Thus, in this simulation, the value of  $F_{roll}$  and  $C_{aero}$  is tuned.

When sorting through the step responses taken at Crow’s Landing, it is apparent that there is discrepancy between the two testing directions, northbound and southbound. Figure 2.2 shows two sets of velocity data collected from the same step input, one in each direction. Other sets of data show this discrepancy as well, and are all corrected accordingly by instating a road grade of 0.12 degrees. In theory, wind disturbance can also contribute to the velocity discrepancy between the two directions, but its inconsistent nature makes it inconvenient to consider it during tuning.

With the small but significant factor of road grade in place, tuning can be done on  $F_{roll}$  and  $C_{aero}$ . During tuning, it is useful to examine the percent error signal. Errors in  $F_{roll}$  will create more of a constant error shift, while those in  $C_{aero}$  will affect the error signal more at higher speeds. Final values of these parameters are listed in Table 2.1.

### 2.1.3.2 Unlocked Vehicle Dynamics

In order to simulate the low-speed regions of the step response, a torque converter model must be simulated. In order to identify the parameters in Equations 2.5 and 2.6, values for  $\tau_{pump}$  and  $\tau_{turb}$  must be available. This information is not currently available on the JBus interface, so it must be calculated from other data. Starting with  $\tau_{pump}$ , rearranging Equation 2.7 yields

$$\tau_{pump} = \tau_{eng} - I_e \dot{\omega}_e \quad (2.9)$$

Engine torque is available directly from the JBus, as is engine speed. Thus by differentiating engine speed, Equation 2.9 can be used to obtain a signal for  $\tau_{pump}$ .

Similarly,  $\tau_{turb}$  can be found by rearranging Equation 2.8:

$$\tau_{turb} = \frac{\dot{v}}{R_g h} \left[ R_g^2 (6I_{wheel} + mh^2) + I_{eng} \right] + R_g \left[ mgh \sin \theta + \tau_{brake} + F_{roll} h + (v + v_{hw})^2 C_{aero} h \right] \quad (2.10)$$

By differentiating vehicle speed (acceleration is not available on JBus) and plugging in the parameters found in the simulations for the locked mode, a signal for  $\tau_{turb}$  is obtained. To handle the problems with noise associated with numerical differentiation, only every tenth data point of engine and vehicle speed were used.

The torque signals are then used to make fits of Equations 2.5 and 2.6, taking  $\omega_p$  to be the same as engine speed, and  $\omega_t$  as the input shaft speed to the gearbox. Both of these speeds are available through the JBus. Using Excel to perform least squares fits, the torque converter parameters are obtained. Figure 2.3 shows the pump torque fit on a torque signal acquired from the 28% throttle step response. The fits are divided into two sections, the uncoupled mode when  $\omega_t/\omega_p$  is less than 0.9, and the coupled mode when  $\omega_t/\omega_p$  is greater or equal to 0.9.

Figure 2.3 shows the fit of one particular torque signal generated from a step response. However, this is only one of a number of torque signals that are fit simultaneously, one of a number of signals from different step responses that span the range of accelerator inputs. In this manner the resulting fits

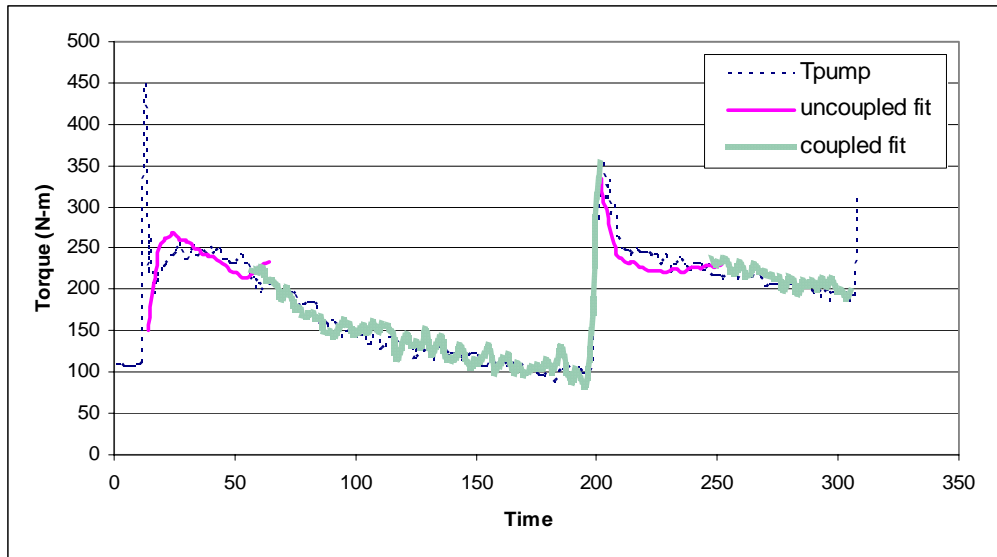


Figure 2.3: Sample Fit of Calculated Pump Torque

become more versatile, and can be applied throughout the whole range of accelerator inputs.

When testing the torque converter model, it is important to first simulate one half at a time. For instance, when simulating to verify the pump torque parameters, the wheel speed data is fed into the simulation. Conversely, when simulating to verify the turbine torque parameters, the engine speed data is fed imported. This way, any errors in the fits can be identified more clearly—it is known which side of the torque converter the errors lie. Only after these steps are taken, both sides of the torque converter can be simulated simultaneously.

## 2.2 Gear Shift

The compressed natural gas engine is mated to a six-speed hydrodynamic automatic transmission, the Allison B400R. The changes in gear shifts for the bus are dependent only speed. The shifting characteristics may change with dramatic changes in road grade, but they stayed consistent with speed even with changes in throttle input and the small road grades present in the airfield

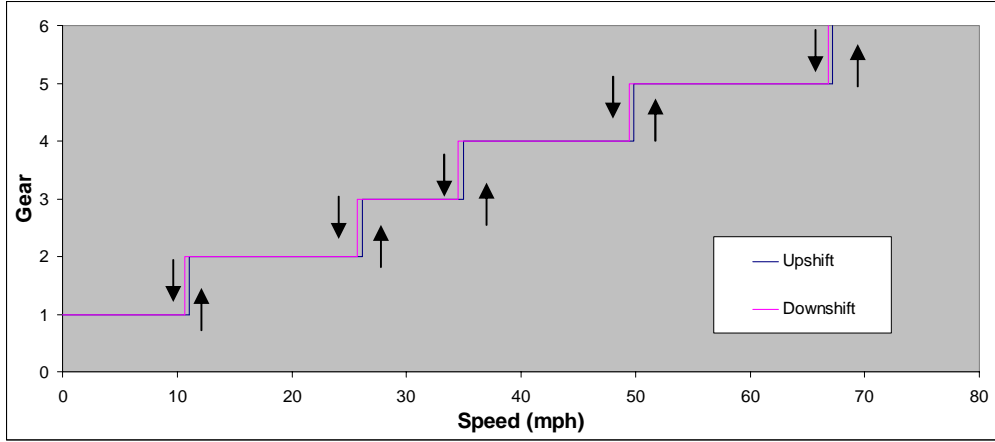


Figure 2.4. Gear Shifting Points

Gear	1	2	3	4	5	6
Ratio	0.287	0.538	0.709	1.00	1.33	1.54

Table 2.3: Gear Ratios

at Crow’s Landing. These shifting speeds are diagrammed in Figure 2.4, and the gear ratios in Table 2.3. Note that gear six is never reached because this particular bus is limited to 64.8 miles per hour.

Note how there is a hysteresis effect in gear shift points; shifting speeds are higher for upshifts than they are for downshifts. This is present to reduce “chatter” in the shifting patterns, i.e. when vehicle speed is hovering around one of the shift points.

Power is sent through a final gear in the differential, with a ratio of 0.189, and thus the overall gearing,  $R_g$ , will be the product of the selected gear ratio in Table 2.3 and the final gear. In order for smooth shifts, gear ratio changes are not instantaneous. In simulation, the gear ratio signal is modeled as a first-order lag system. In Equation 2.11,  $R_s$  represents the selected gear ratio, while  $\tau_g$  is tuned to 0.5 seconds.

$$\dot{R}_g = \frac{1}{\tau_g} (-R_g + R_s) \quad (2.11)$$

## 2.3 Engine

Detailed thermodynamic models of CNG engines have been developed [5][6] but examining the intricacies of the engine block and obtaining the numerous model parameters is beyond the scope of this modeling study. To obtain a useable model of the CNG engine for simulation, it is sufficient to know how much torque the CNG engine is producing. The torque characteristics of the CNG Engine are modeled as a two-dimensional map

$$\tau_{map} = \tau_{map}(\omega_e, TI) \quad (2.12)$$

which states that the torque produced by the engine,  $\tau_{map}$ , is a nonlinear function of the current engine speed,  $\omega_e$ , and the throttle input,  $TI$ , a percentage value. Since the bus's throttle is actuated electronically, the throttle can be controlled directly without worry of pedal angles.

With the step response data acquired at Crow's Landing, it is possible to develop the engine map one layer at a time by observing how engine torque varies with engine speed, given the fixed throttle step input. When examining each 'slice' of the torque map in this matter, it becomes quickly evident that having one map will be insufficient to characterize the bus engine at all times.

Figure 2.5 shows a typical engine speed versus torque plot, and it can be seen that first gear has a different torque curve than the rest of the gears in the step response, which in this case are gears two through five. All step responses tested show this characteristic. Thus, two separate torque maps are developed: one for first gear, and one for the other gears. Graphically, Figure 2.6 shows the torque maps for first gear (a), and the higher gears (b).

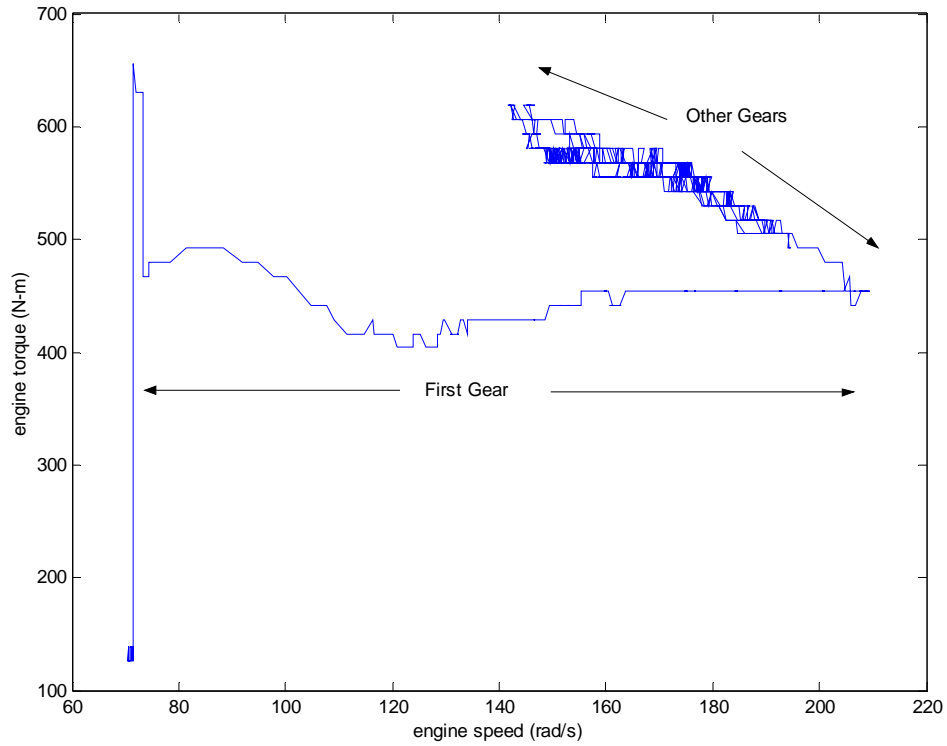


Figure 2.5: Engine Speed and Torque at Constant 38.78% Throttle Input

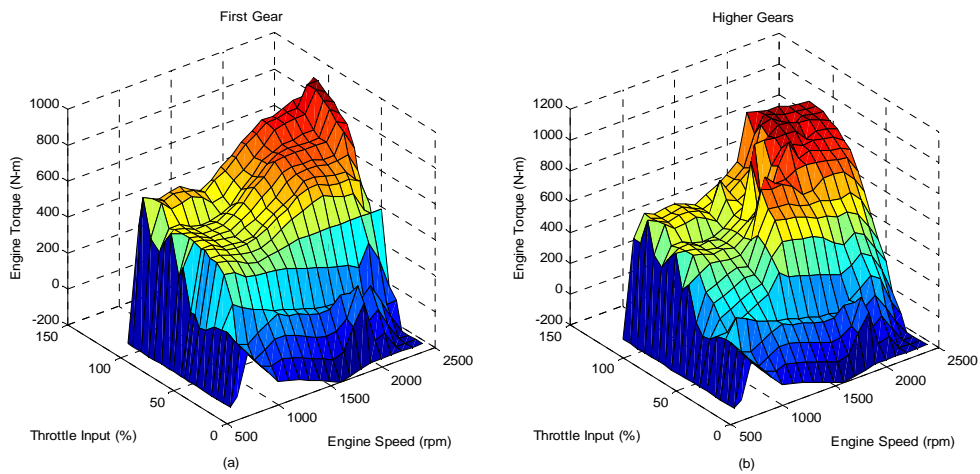


Figure 2.6: Engine Maps for (a) First Gear and (b) Higher Gears

Engine Speed (RPM)	Gross HP	Net HP	$P_{loss}$ (HP)
1300	207.9	197.0	10.9
1400	226.6	214.6	12.0
1500	235.9	222.7	13.2
1600	244.3	229.8	14.5
1800	258.8	241.0	17.8
2000	269.2	247.5	21.7
2200	276.5	250.0	26.5
2400	280.0	247.8	32.2

Table 2.4. Accessory Loss Power Ratings [2]

Only a part of  $\tau_{map}$  traverses the driveline and makes its way into the overall vehicle dynamics, due accessory torque losses and driveline losses. Given accessory horsepower losses of the engine at different engine speeds [2], a mapping of torque losses in terms of engine speed is possible with the following relationship:

$$\tau_{acc}(\omega_e) = \frac{P_{loss}(\omega_e)}{\omega_e} \quad (2.13)$$

$\tau_{acc}$  is the torque lost to the accessories, and  $P_{loss}$  is the power rating. Table 2.4 reproduces the gross horsepower and net horsepower ratings at different engine speeds. The differences between these ratings are  $P_{loss}$  values. In simulation these values are interpolated to create a nonlinear mapping between engine speed and  $\tau_{acc}$ . Incorporating driveline efficiency, the total net engine torque transmitted through the driveline is

$$\tau_{eng} = (\tau_{map} - \tau_{acc}) \cdot \epsilon_{driveline} \quad (2.14)$$

where  $\epsilon_{driveline}$  is the driveline efficiency, 0.9613.

## Chapter 3

### Simulation Analysis

The performance of the resulting model is investigated in this section. The simulations will be presented in order of increasing complexity: at first only the vehicle dynamics will be simulated, then gear shifts will be added, then engine torque. When gear shifts and engine torque are not simulated, they are simply read in from the JBus data values. The figures presented in this section are all simulated only with the 98.4% step response in the interests of concision, but are characteristic of other step responses as well. Finally, the section will conclude with a segment describing possible future work that could be done to improve these results.

#### 3.1 Vehicle Dynamics

Figure 3.1 shows a characteristic step simulation with vehicle dynamics (gear shifts and torque are from data). The vehicle speed (a), engine speed (b), and their percent errors (c) are all shown. The solid vertical black line in all 3 plots indicates when locking of the torque converter occurs.

Errors in both velocity and engine speed are generally well within 10%. The worst errors come in to play at low speeds, when the torque converter is unlocked. The velocity error is generally worse in this region because the reference velocity is low, and dividing by this data results in error magnification. The engine speed in this region is more accurate because more torque is involved on that side of the torque converter, resulting in a less sensitive simulation. Also, the low speeds and torques in general make the unlocked dynamics more sensitive to disturbances (road grade, wind) and modeling errors. In the locked region of the response, the errors of both engine speed and vehicle speed are very similar, because the locked torque converter

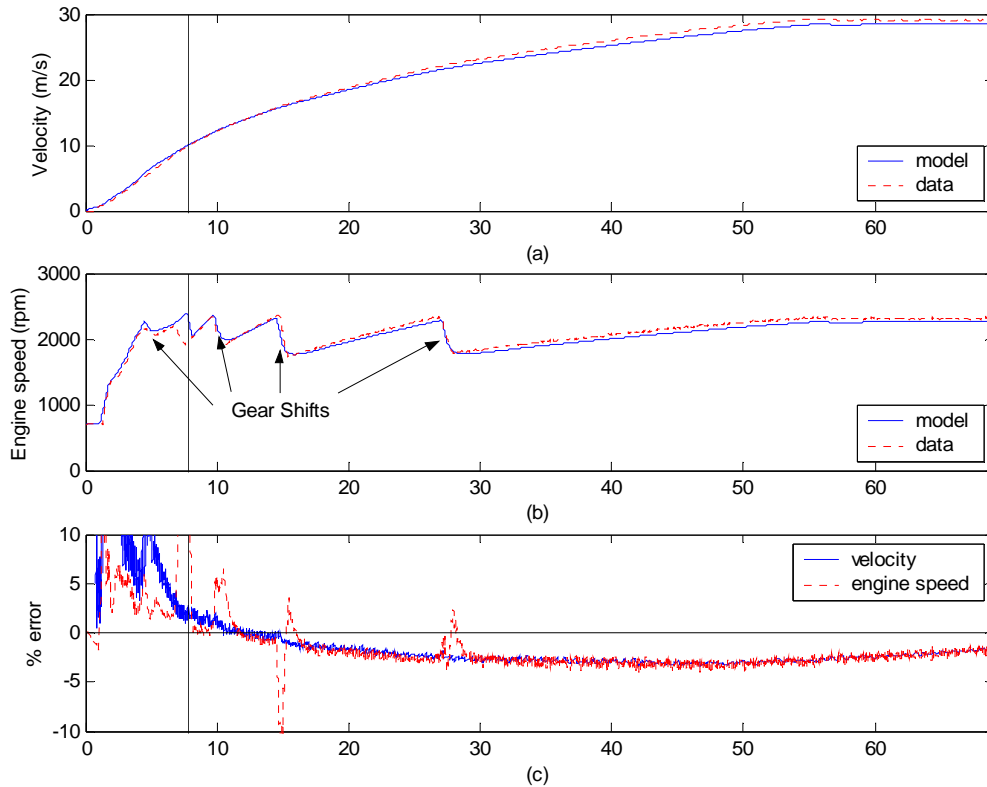


Figure 3.1: Step Response with Vehicle Dynamics Simulation

means a direct ratio between the two. The only differences in the error signal come at places where the gear shifts occur, where small spikes in the engine speed occur from this highly sensitive region.

## 3.2 Vehicle Dynamics and Gear Shifts

Figure 3.2 shows the same step input but this time with the shift points commanded by the simulation, not by JBus data. While the velocity profile stays relatively unchanged, the engine speed signal suffers larger discrepancies around the shift points. This can be seen best in the shift from fourth gear to fifth gear in plot (b). The engine speed simulation differs from the data by about only two percent, but creates a large error for nearly two seconds. This

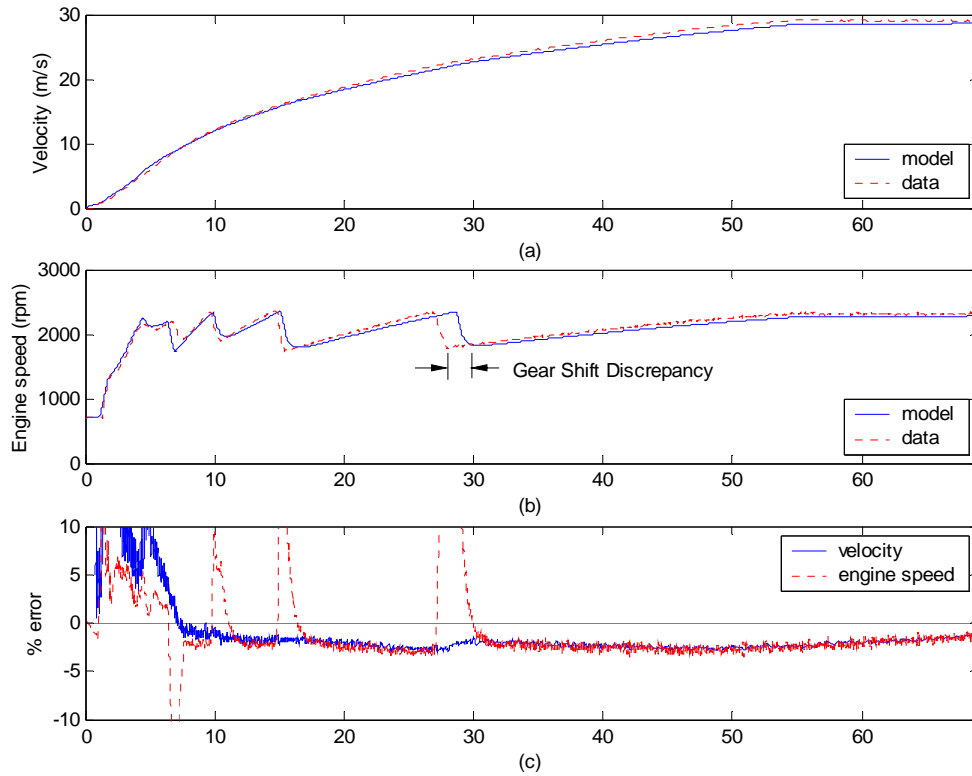


Figure 3.2: Step Response with Vehicle Dynamics and Gear Shift Simulation

is because the shifts are dictated by speed, and the acceleration at the end of fourth gear is not great, so the two second lag is apparent. Due to the highly volatile nature of engine speed due to gearing, vehicle speed is usually a more accurate simulation.

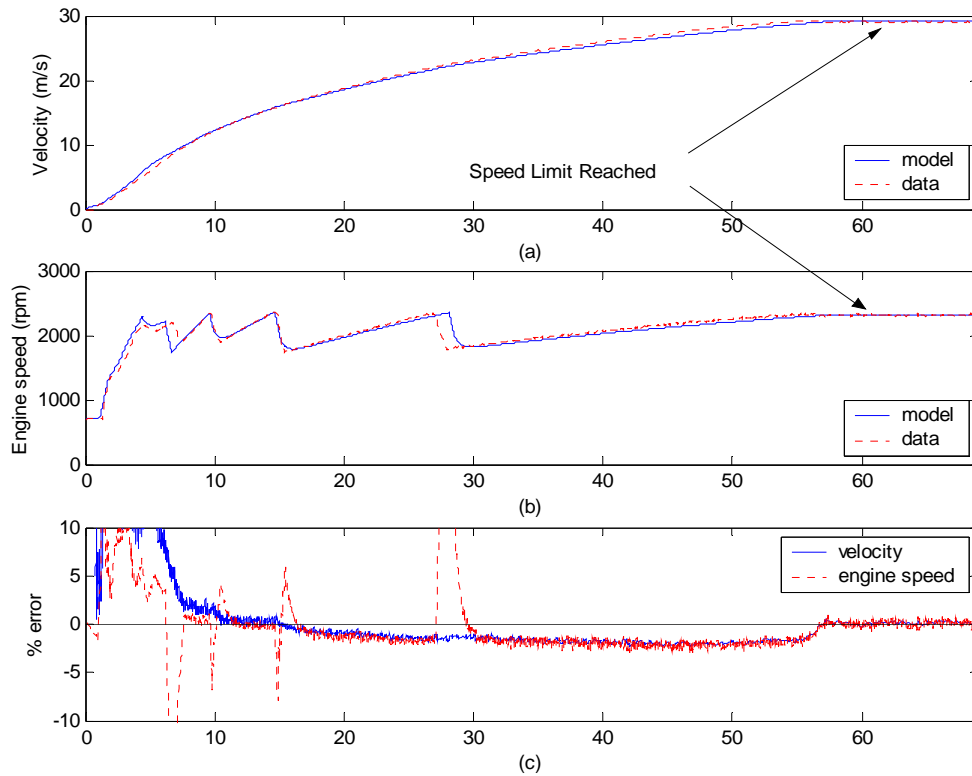


Figure 3.3: Step Response with Full Simulation

### 3.3 Complete Simulation (VD, Gear Shifts, Torque Mapping)

By replacing the torque values from the JBus with values generated by the torque maps, a complete simulation is now attained. That is, the only input is the pedal position; engine torque, gear shifts, and unlocked and locked vehicle dynamics are all completely simulated. Figure 3.3 displays the results of the same step response as before, but with this full simulation.

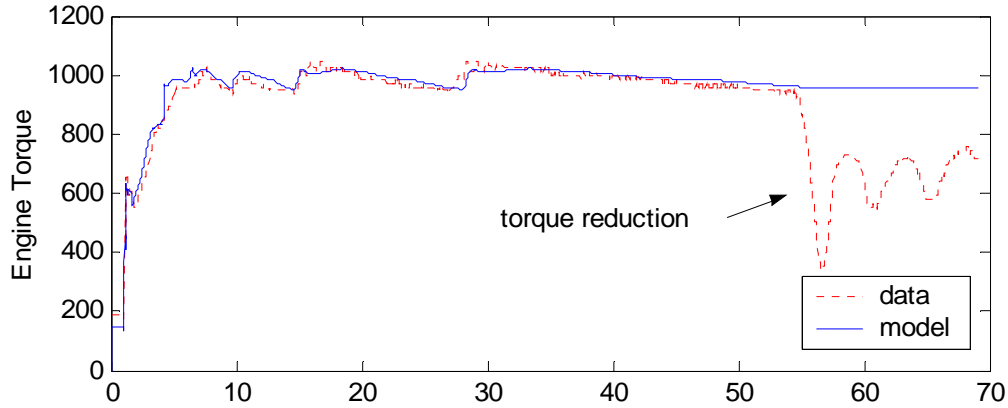


Figure 3.4: Torque Signals for the 98.4% Step Response

The torque map matches reality fairly well. As a result, the simulation is again accurate, with only slightly more error occurring in the unlocked region, where sensitivity to torque errors are greater. Also, note that the limit in vehicle speed was reached. In Simulink, the speed limit was modeled as a saturation. This works fine for simulation, but does not give an accurate representation of the torque that was actually produced during that time.

### 3.4 Future Work

In Figure 3.3, the speed was limited in simulation simply by entering in integration limits in the vehicle acceleration integrator in the locked dynamics (Equation 2.1). In reality, the bus computer enforces the speed limit by reducing the engine torque output when the limit has been reached. Figure 3.4 illustrates how the real torque data is lowered in the final seconds of the run to keep the speed from overcoming the limit. Future work could be done to develop the speed governor model, and how the torque is modified to govern speed. Other areas that could be investigated in future work are the dynamics involved in slowing down: engine retarder and brake dynamics.

Better instrumentation can also be done on the buses, so that more data is available for analysis. For instance, wind meters could be mounted on the bus to measure relative wind velocities, and electronic levels could measure

road grade. Road grade contributes a lot to the dynamics of the vehicle, even at very small angles (Figure 2.2). Finally, torque converter parameter identification would be greatly helped if pump and turbine torques can be measured directly. This would eliminate the noise and inaccuracies involved in differentiating engine and vehicle speed.

## Chapter 4

### Summary and Conclusions

The more accurate a model, the better a control system can be developed for the physical system it represents. Presented in this paper was a working simulation model of the 40 foot New Flyer Bus powered by a Cummins CNG engine. The model was divided and presented in three sections: vehicle dynamics, gear shifts, and engine torque dynamics. Along with the model, the methodology used to tune and come about model parameters was also given. Then this paper examined the model in action, comparing the simulated model against actual driving data.

It can be seen that the low-speed dynamics of the bus are the most complex aspect of the model. At low speeds, the bus is the most sensitive to wind and road grade disturbances, and the simulation is most prone to error. This is the result of the complexities of the unlocked torque converter, and the different engine map used in first gear. Inaccuracies in gear shifting have little effect on the velocity of the vehicle, but give large spikes of error in the engine speed signal. Thus, it is more desirable to control a vehicle by vehicle speed, rather than by engine speed. It was shown that this model can be used to accurately predict the vehicle acceleration speed to within 5% error in locked torque converter mode, and generally 10% in unlocked torque converter mode. In the unlocked mode, engine speed develops less percent error than vehicle speed, due to the greater torques involved and a better parameter fit. Lastly, having data available to be fed in to the simulations is useful for isolating certain components of the model during the tuning process. Similarly, during controller implementation, having data available directly from the JBus will give the operators better understanding of the bus behavior, and lead to better control.

# Bibliography

- [1] J.K. Hedrick. PATH RFP for 2002-2003: Vehicle Modeling and Verification of CNG-Powered Transit Buses. 2003.
- [2] Allison personal contact. SCAAN No 710715. 2003.
- [3] B. Song, J.K. Hedrick, A. Howell. Fault Tolerant Control and Classification for Longitudinal Vehicle Control. *ASME Journal of Dynamic Systems, Measurement, and Control*, 2003.
- [4] D. Cho, J.K. Hedrick. Automotive Powertrain Modeling for Control. *ASME Journal of Dynamic Systems, Measurement, and Control*, 1989.
- [5] A. Gangopadhyay and P. H. Meckl. Modeling, validation and system identification of a natural gas engine. *In the American Control Conference*, pages 294-298, Albuquerque, NM, June 1997.
- [6] A. Gangopadhyay and P. H. Meckl. Extracting physical parameters from system identification of a natural gas engine. *IEEE Transactions on Control Systems Technology*, 9(3):425-434, May 2001.